J Radioanal Nucl Chem (2017) 312:717–723
DOI 10.1007/s10967-017-5193-2

# Visualization of how light changes affect ion movement in rice plants using a real-time radioisotope imaging system

**Ryohei Sugita[1] · Natsuko I. Kobayashi[1] · Atsushi. Hirose[1] · Ren Iwata[2] · Hisashi Suzuki[3] · Keitaro Tanoi[1,4] · Tomoko M. Nakanishi[1]**

Received: 17 June 2016 / Published online: 13 February 2017


**Abstract** We developed a real-time radioisotope imaging system (RRIS) technique that can nondestructively visualize the element absorption and transport process in plants, using not only positron emitters but also commercially available radioisotopes. In this study, we applied RRIS to analyze light effects on ion movement in rice plants. As tracers, $^{28}$Mg, $^{32}$P, and $^{45}$Ca were used. During the first 5 h, dark/light cycle of 3/7 min were set up; the RRIS needs dark conditions during capturing. When the light was ceased 5 h after supplying each tracer, $^{32}$P transport from root to shoot decreased immediately. In contrast, $^{28}$Mg and $^{45}$Ca transport did not change with light conditions. These results suggest that the P transport is dependent on water flow, whereas Mg and Ca transport are independent of water flow.

**Keywords** Mineral elements · Transport · Transpiration · Live imaging · Real-time radioisotope imaging system

**Electronic supplementary material** The online version of this article (doi:10.1007/s10967-017-5193-2) contains supplementary material, which is available to authorized users.

✉ Keitaro Tanoi
uktanoi@g.ecc.u-tokyo.ac.jp

[1] Graduate School of Agricultural and Life Sciences, The University of Tokyo, 1-1-1, Yayoi, Bunkyo-ku, Tokyo 113–8657, Japan

[2] Cyclotron and Radioisotope Center (CYRIC), Tohoku University, 6-3, Aoba, Aramaki, Aoba-ku, Sendai, Miyagi 980-8578, Japan

[3] National Institute of Radiological Sciences, 4-9-1, Anagawa, Inage-ku, Chiba-shi, Chiba 263-8555, Japan

[4] PRESTO, Japan Science and Technology Agency (JST), 4-1-8 Honcho, Kawaguchi, Saitama 332-0012, Japan

## Introduction

Increased food production is one of the most important issues worldwide, particularly in regions where population growth is anticipated, for example in Asia and Africa. Water, nutrients, and light are essential for plant growth. The improvement of yield using technology that reduces fertilizer is indispensable. For effective fertilization, it is necessary to understand the mechanism behind ion transport and distribution in plants. There are two pathways facilitating long distance ion transportation within plant tissues, namely xylem and phloem. After ions cross the epidermal tissue of the root, they move across the root cells and enter the xylem vessels, where the upward flow of ions together with water is observed. The main driving force of water is a water potential gradient produced by transpiration and root pressure and built up by the active secretion of ions to the vascular tissues [1]. Transpiration is affected by photoenvironment; it decreases several minutes after the transition from light to dark [2], which immediately reduces the water flow in xylem [2, 3]. The phloem flow transports ions, photosynthetic products, and water from the source tissues, such as mature leaves, to the developing young tissues, the so-called "sinks." The water flow along the phloem sieve tubes is powered by the active transmembrane transport of sucrose at the source organ, which generates turgor pressure differences between source and sink sites [4]. These water flows are supposed to affect the transport of various solutes through the vasculature, including ions, although the actual relationships remain incompletely understood. Indeed, several reports have indicated the complex and solute-specific mechanisms underlying the long distance transport through xylem and phloem. Biddulph et al. revealed that the longtitudinal transport velocity of phosphorus was the same as that of

water [5]. When compared with sugars and amino acids, water molecules were shown to escape from xylem vessels easily, following which they re-enter the vessels continuously during the xylem transport process [6–8]. It is also obvious that the behaviors of ions during the long distance transport differ from each other [9, 10]. To understand the mechanisms regulating ion transport through the vasculature, identifying the factors affecting the transport of each ion is important. Here, we have evaluated the effect of photoenvironment on the transport kinetics of phosphate, magnesium ($Mg^{2+}$), and calcium ions ($Ca^{2+}$) in rice plants via radiotracer experiments.

## Experimental

### Test plants

Rice plants (*Oryza sativa*. L. "Nipponbare") of 8-day old were used as test plants. At this age, the fourth leaves of the plants were about to emerge. Rice seeds were grown in 0.5 mM $CaCl_2$ solution under dark conditions for 2 days. Then, rice plants were transplanted and cultured in a half-strength Kimura-B nutrient solution for 4 days under 16/8 h light/dark conditions. All day, the temperature and the humidity were 30 °C and 70%, respectively. During daytime, the photosynthetic photon flux density was 100 μmol $m^{-2}$ $s^{-1}$. The concentrations of the chemicals in the solution was: 180 mM $(NH_4)_2SO_4$, 270 mM $MgSO_4$, 91 mM $KNO_3$, 180 mM $Ca(NO_3)_2$, 91 mM $KH_2PO_4$, 46 mM $K_2SO_4$, 46 mM Fe-citrate, 6.7 mM $MnCl_2$, 9 mM $H_3BO_3$, 150 nM $ZnSO_4$, 160 nM $CuSO_4$ and 15 nM $(NH_4)_6Mo_7O_{24}$. The pH was kept to 5.6 using 2.5 mM 2-morpholinoethanesulfonic acid (MES) [11].

### Distribution of $^{28}$Mg, $^{32}$P, and $^{45}$Ca

About five plants were placed under light conditions (100 μmol $m^{-2}$ $s^{-1}$), besides others were placed under dark conditions. $^{32}$P and $^{45}$Ca are commercially available radioisotopes (PerkinElmer, Inc. MA, USA). The short half-life radionuclide, $^{28}$Mg, was produced using a cyclotron through a $^{27}$Al(α 3p) $^{28}$Mg reaction [12]. The characteristics of the three radionuclides were listed in Table 1. $^{28}$Al is a daughter of $^{28}$Mg. These radiation energies emitted from each radionuclide greatly varied, therefore influence of the self-absorption varies according to a radionuclide [13]. So in this case, it was difficult to compare the radionuclides activity among different tissues, especially in the case of relatively weak beta ray emitter, like $^{45}$Ca. So we analyze the data semi-quantitatively. Each radioactive tracer was applied to the roots in half-strength Kimura-B nutrient solution. The tracer concentrations were as follows: $^{28}$Mg: 8.3 kBq $mL^{-1}$; $^{32}$P: 8.3 kBq $mL^{-1}$; and $^{45}$Ca: 83 kBq $mL^{-1}$. After 5 h absorption of radiotracer, the accumulation of $^{28}$Mg, $^{32}$P, and $^{45}$Ca signals within shoots and roots, respectively, was measured using ImagingPlate (IP; BAS-IP MS, GE Healthcare, Buckinghamshire, UK) and a FLA-5000 image reader (FujiFilm, Tokyo, Japan).

### Visualization of element movement

The visualization was performed using a real-time radioisotope imaging system (RRIS) [9, 14]. In brief, radiation emitted from radioactive tracers in a sample was changed to light by a fiber optic plate with a CsI (Tl) scintillator (FOS), following which the light was captured by a charge coupled device (CCD) camera (AQUA-COSMOS/VIM system, Hamamatsu Photonics Co., Hamamatsu, Japan) [13]. Four plants were placed in a root chamber containing nutrient solution. The root chamber comprised a polyethylene bag and a blue polyurethane sheet (Fig. 1a). The roots were fixed using the polyurethane sheet. The root chamber was then pressed onto the scintillator using acrylic resin plates (Fig. 1b). The leaves were fixed on the scintillator using medical tape. Each radioactive tracer was applied to the roots. The activities of the supplied nuclides were as follows: $^{28}$Mg: 17 kBq $mL^{-1}$; $^{32}$P: 30 kBq mL; $^{-1}$and $^{45}$Ca: 830 kBq $mL^{-1}$. The tracer concentrations between RRIS and IP (described above "Distribution of $^{28}$Mg, $^{32}$P, and $^{45}$Ca") were set differently. All tracer images were taken by RRIS for 10 h. Two states of photoenvironment were used: 5 h light conditions and 5 h dark conditions. During the first 5 h, light emitting diodes (LEDs) (100 μmol $m^{-2}$ $s^{-1}$) with a dark/light cycle

**Table 1** General overview of the radionuclides used in this study

| Nuclide | Mode of decay | Half-life | β-ray Maximum energy (keV) | γ-ray energy (keV) |
|---|---|---|---|---|
| $^{28}$Mg | $\beta^-$ | 20.9 h | 860 | 1589 |
| $^{28}$Al | $\beta^-$ | 2.2 min | 2863 | 1779 |
| $^{32}$P | $\beta^-$ | 14.3 days | 1711 | – |
| $^{45}$Ca | $\beta^-$ | 163 days | 257 | – |

The $^{28}$Al is daughter nuclide of $^{28}$Mg

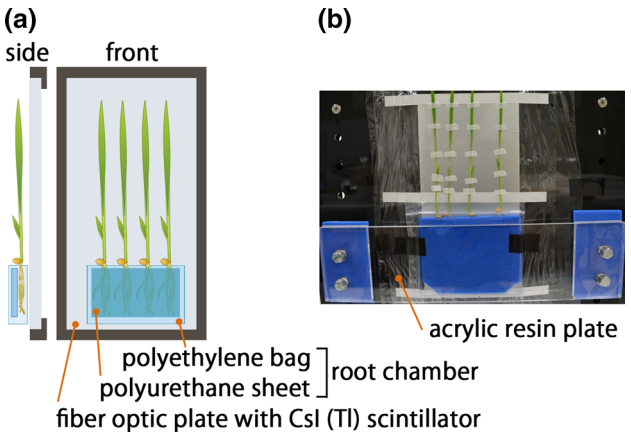


**Fig. 1** The test plant arrangement in RRIS (real-time radioisotope imaging system). **a** Schematic image of a root chamber. **b** Photograph of a plant and root chamber arrangement

of 3 min/7 min were set up. The RRIS images were taken during the dark period to protect the highly sensitive CCD camera [15]. During the next 5 h, the RRIS images were acquired for 3 min every 10 min. Therefore, 30 pictures were obtained in each of the first and second 5 h (total 60 pictures). The RRIS provided images of radiotracer distributions among roots and shoots, and successive images were sequentially stacked into a movie. Based on the images, the uptake and the shoot transportation of each ion were analyzed by the measurement of signal intensities in the region of interest (ROI) (Fig. 3a). All shoot part as a ROI from which the background (obtained from an area in that ROI with no leaf or stem) was then subtracted. After the ROI intensities were subtracted from that of the background, the time course of signal intensity within the ROI was obtained as the increment in intensity relative to the first image frame, which was supposed to be derived from the simple adherence on the root surface by the nuclides.

### Transpiration rate

Transpiration rate was calculated as decrement of the culture water either under light conditions for 10 h, or under light conditions for 5 h followed by 5 h of dark conditions. Here, the light conditions indicates the intermittent light conditions using LEDs (100 μmol $m^{-2}$ $s^{-1}$), which was adopted for visualization of elements. Test plant was set as described above "Visualization of element movement". One sample was composed of four plants, and four samples were calculated. The samples without a plant were set in both the light conditions and dark conditions to evaluate quantity of direct evaporation of the culture water.

## Results and discussion

### Distribution of $^{28}$Mg, $^{32}$P, and $^{45}$Ca

To quantitatively analyze the influence of the photoenvironment on ion movement, the radioactivity of $^{28}$Mg, $^{32}$P, and $^{45}$Ca within the shoots and roots after light or dark periods was measured by radioluminography using IP. As a result, $^{28}$Mg, $^{32}$P, and $^{45}$Ca absorption from roots was not influenced by the light (Table 2), even though water but also ions can be transported in the xylem and the phloem also during darkness [16]. In particular, no change in the movement from root to shoot was detected for $^{45}$Ca. Thus, $Ca^{2+}$ is supposed to be absorbed and transported independently from water flow. On the other hand, dark treatment decreased $^{28}$Mg and $^{32}$P movement from root to shoot from 3.6 to 2.4 and from 11 to 4.8 potostimulated luminescence (PSL) $\mu g^{-1}$ shoot fresh weight (FW), respectively (Table 2). PSL is proportional to the amount of radioactivity. As a result, the shoot–root ratio under dark condition relative to shoot–root ratio under light condition of $^{28}$Mg and $^{32}$P were 0.59 and 0.57, respectively (Table 2). These results show that light can promote the flow of $Mg^{2+}$ and phosphate through xylem. Thus, it could be hypothesized that $Mg^{2+}$ and phosphate were mainly transported in the flow of water through the xylem. Another possibility is that photosynthesis and metabolism under a light condition might maintain energy generation, which could be required for long distance transport of $Mg^{2+}$ and phosphate, regardless of the water flow.

### Analysis of $^{28}$Mg, $^{32}$P, and $^{45}$Ca movement

To examine the impact of water flow on ion transport, the dynamics of ion movement in response to the transition between photoenvironments was monitored using RRIS. In the present experiment, each nuclide, $^{28}$Mg, $^{32}$P, and $^{45}$Ca, was supplied to roots and visualized for 0–5 h under a light condition and then for 5–10 h under a dark conditions (Fig. 2a–c). Based on the successive images (Online Resource 1), the time courses of each nuclide accumulation were obtained (Fig. 3b–d). Figure 3e was the time courses of $^{32}$P under 10 h under a light condition. It was shown that accumulation was first observed in the root, followed by accumulation in the shoot for all three ions (Fig. 3b–d). Nevertheless, when observing the $^{45}$Ca accumulation process, accumulation within roots was shown to be almost saturated before approximately 3 h, whereas accumulation to the shoot continued to increase (Fig. 3d). It could be suggested that the turnover for $Ca^{2+}$ in root tissues, including ion exchage at the inner-surface of xylem vesseles [17], is rapid, and surplus $Ca^{2+}$ is probably

**Table 2** Ion accumulation in roots and transportation to shoots under light/dark conditions (PSL $\mu g^{-1}$ root fresh weight (FW)). Relative shoot/root shows the shoot–root ratio relative to the shoot–root ratio under light condition; ((shoot PSL)/(root PSL))/((shoot/PSL of light))/(root PSL of light)). Each value is tabulated as the mean ± standard deviation. PSL means photostimulated luminescence. PSL is proportional to the amount of radioactivity. The *p*-values between light and dark were examined by *t* test

| | | Whole plant | | Shoot | | Root | | Relative shoot/root | |
|---|---|---|---|---|---|---|---|---|---|
| | | (PSL/μg whole plant FW) | *p*-value | (PSL/μg shoot FW) | *p*-value | (PSL/μg root FW) | *p*-value | $\frac{(\text{shootPSL})/(\text{rootPSL})}{(\text{shoot PSL of light})/(\text{root PSL of light})}$ | *p*-value |
| $^{28}$Mg | Light | 3.9 ± 0.55 | 0.080 | 3.6 ± 0.44 | 0.00082 | 4.5 ± 1.5 | 0.42 | 1.0 | 0.0071 |
| | Dark | 3.4 ± 0.37 | | 2.4 ± 0.49 | | 5.2 ± 1.4 | | 0.59 ± 0.29 | |
| $^{32}$P | Light | 15 ± 8.3 | 0.51 | 11 ± 4.0 | 0.0036 | 41 ± 11 | 0.15 | 1.0 | 0.0053 |
| | Dark | 12 ± 2.6 | | 4.8 ± 1.0 | | 34 ± 7.6 | | 0.57 ± 0.28 | |
| $^{45}$Ca | Light | 2.0 ± 0.24 | 0.14 | 2.3 ± 0.34 | 0.10 | 1.0 ± 0.17 | 0.27 | 1.0 | 0.55 |
| | Dark | 1.8 ± 0.17 | | 2.0 ± 0.32 | | 1.2 ± 0.28 | | 0.95 ± 0.21 | |

$n = 5$ or 6

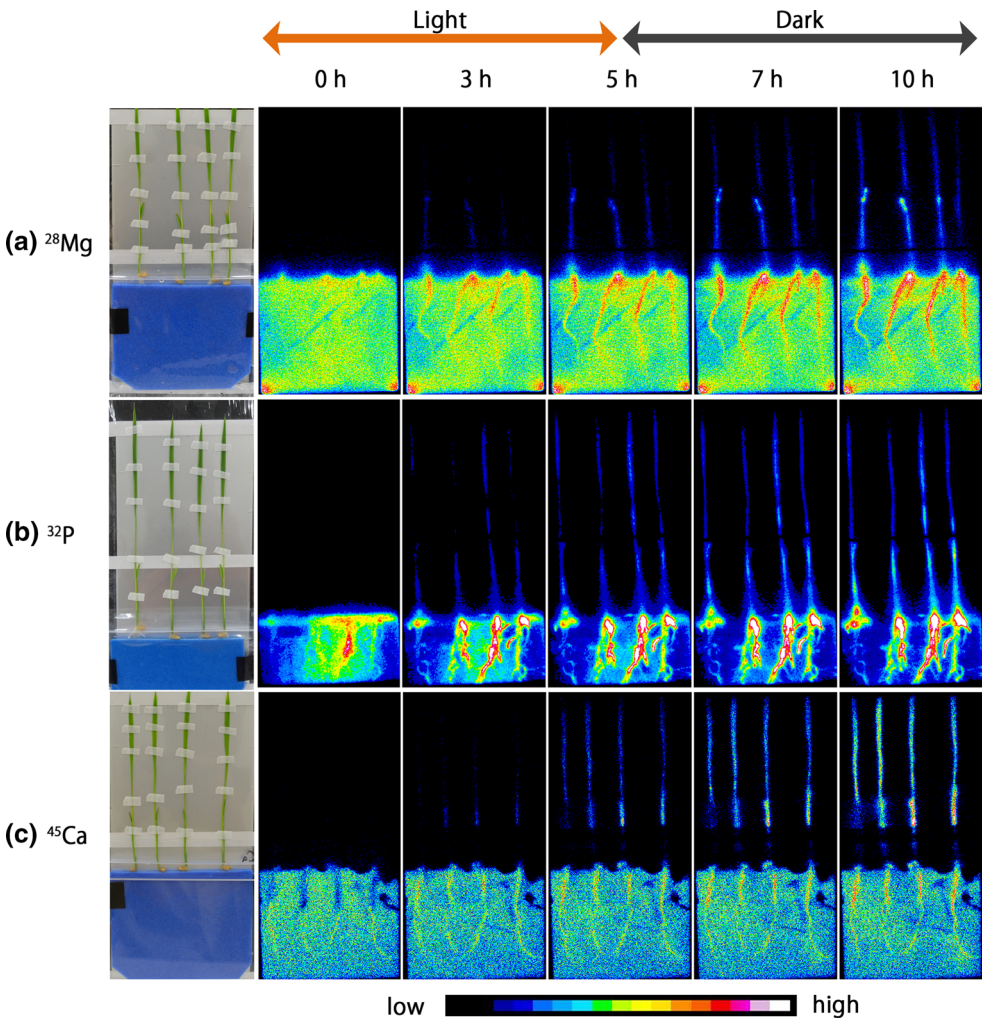


**Fig. 2** Serial images of ion distribution under light/dark conditions in rice, taken by RRIS (real-time radioisotope imaging system). The four test plants were placed in RRIS. Each nuclide of **a** $^{28}$Mg, **b** $^{32}$P, and **c** $^{45}$Ca was supplied to the roots. The activities of the nuclides were as follows: $^{28}$Mg: 17 kBq $mL^{-1}$, $^{32}$P: 30 kBq $mL^{-1}$, and $^{45}$Ca: 830 kBq $mL^{-1}$. After the radioisotope was added, the serial images were taken under light conditions for first 5 h and dark conditions for the following 5 h. The detection time for each image was set to 3 min, and the images were taken every 10 min. The maximum values of *color-bar* were as follows: $^{28}$Mg: 73, $^{32}$P: 440, and $^{45}$Ca: 20. (Color figure online)

transported to the shoot tissues. Another possibility is that when $Ca^{2+}$ moves into the roots and is saturated once, $Ca^{2+}$ is transported to the shoot. To compare the accumulation between each nuclide, the signal intensity based on Fig. 3b–e was normalized at 5 h (Fig. 3f–i). The rate of $^{32}$P accumulation decreased immediately after the

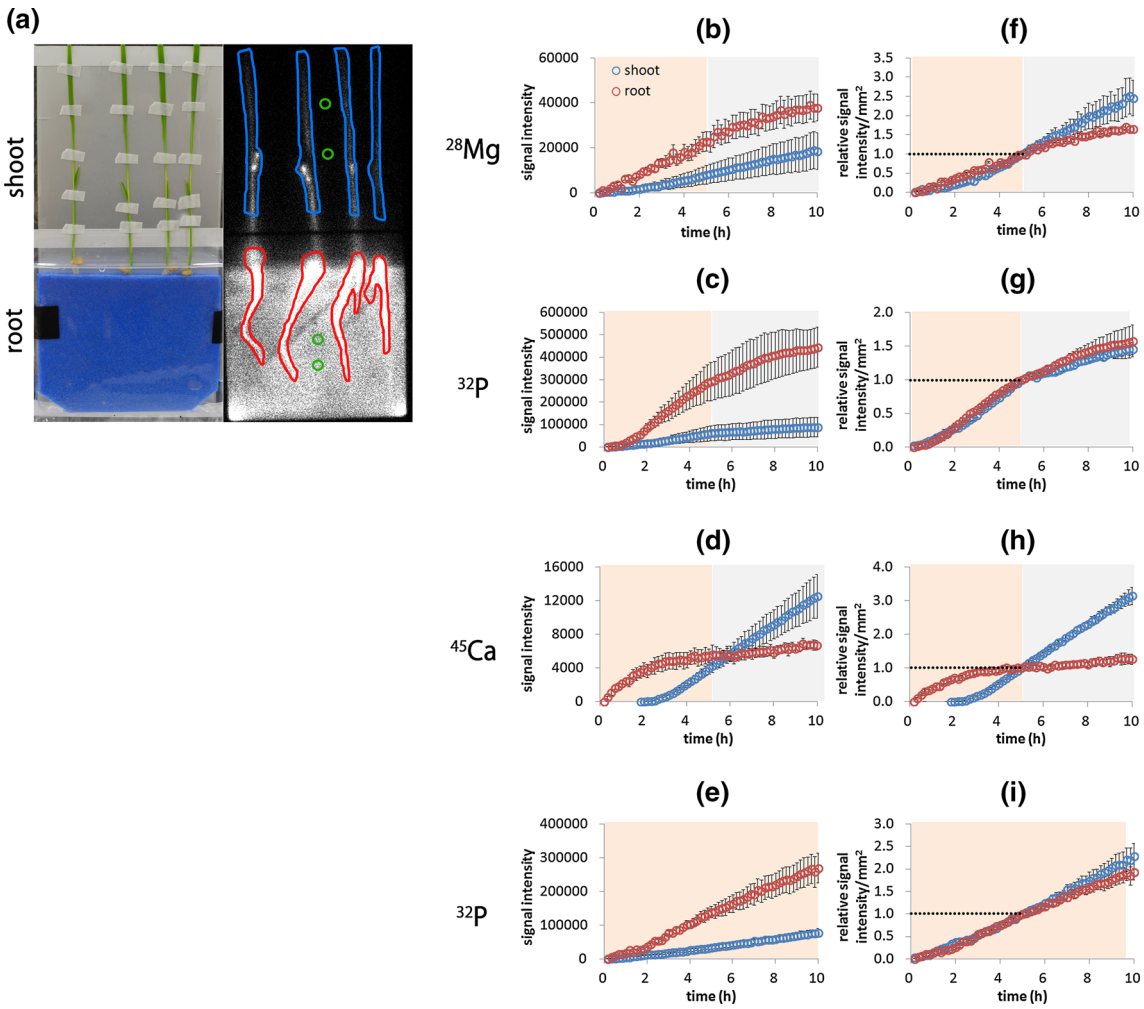


**Fig. 3** The influence of ion movement under light/dark conditions. **a** Photograph of test plants and each ROI is surrounded in the *black* and *white* photograph. The *blue lines*, *red lines*, and *green lines* indicate the ROI of shoot, root, and background, respectively. Time-course analysis of the radioactivity of **b** $^{28}$Mg, **c** $^{32}$P, and **d** $^{45}$Ca, **e** $^{32}$P and the relative signal intensity normalized at 5 h (**f–i**) are shown, respectively. Photoenvironment was under **b–d** light conditions for first 5 h, and dark conditions for next 5 h, **e** light conditions for 10 h. Mean ± standard deviation of four plants are presented. (Color figure online)

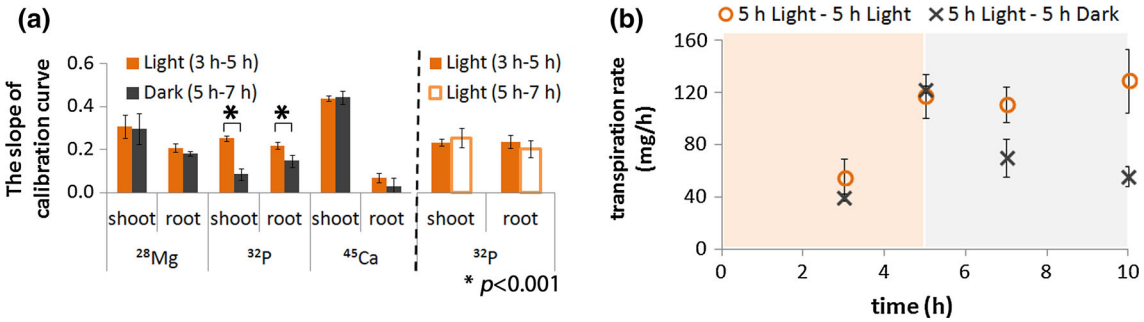


**Fig. 4** **a** The slope of the calibration curve between 3–5 h (*light*) and 5–7 h (*dark*) based on Fig. 3f–h, 3–5 h (*light*) and 5–7 h (*light*) based on Fig. 3i. Mean ± standard deviation of four plants are presented. **b** Transpiration rate was calculated under the light condition for 10 h (*circles*), or under light conditions for 5 h followed by 5 h of dark conditions (*crosses*) at 3, 5, 7 and 10 h. Mean ± standard deviation of four samples in which one sample is composed of four plants are presented

light ceased (Fig. 3g). When the slope of calibration curve in leaves is regarded as the $^{32}$P accumulation velocity, the $^{32}$P accumulation velocity after the light/dark transition was decreased by 66% compared to that before the light/-dark transition (Fig. 4a). Meanwhile, the transpiration rate was decreased by 37% as a consequence of the light-off

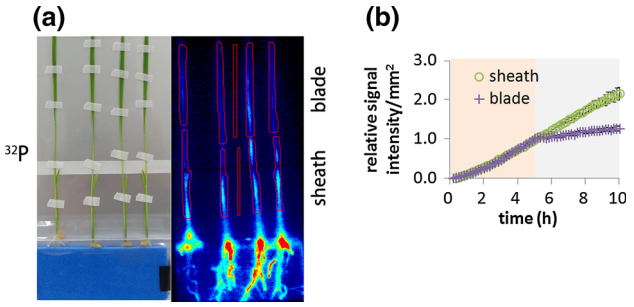


**Fig. 5** The effect of light conditions on P transportation from sheath to blade. **a** The *red boxes* indicate the regions of interest (ROI) in which the signal intensity was determined. **b** Time-course analysis of relative signal intensity $mm^{-2}$ of $^{32}P$ at the blade and sheath. The first 5 h were light conditions and the following 5 h were dark conditions. Mean ± standard deviation of four plants are presented. (Color figure online)

(Fig. 4b). This result suggests that the phosphate absorption and transport is dependent on water flow. Conversely, in $^{28}Mg$ and $^{45}Ca$, the velocity of absorption in roots and transportation to shoots did not change according to the light/dark transition (Fig. 4a). It is suggested that $Mg^{2+}$ and $Ca^{2+}$ transportation from root to shoot is not primarily driven by light. Instead, for $Mg^{2+}$ transport, energy-consuming transmembrane transport processes might be necessary, which could be inactivated during hours of darkness (Table 2).

For the further investigation of the contribution of water flow to phosphate transportation, we sepatated the ROIs between the leaf blade and the leaf sheath (Fig. 5a), because the transpiration activity is high (40–60%) in leaf blade and low (20–35%) in leaf sheath [18]. The accumulation velocity of $^{32}P$ in the sheath was maintained after the transition to the dark period, whereas the $^{32}P$ transport to the blade almost ceased (Fig. 5b). Even if the rate of phosphate flow through the vasculature drops, the amount of phosphate transported to the sheath tissue is constant. Thus, it is suggested that the phosphate unloading mechanism to the sheath is robust, quantitatively regulated, and independent of water flow in xylem (Fig. 5b).

## Conclusions

(1) The live imaging technique, RRIS, is a powerful tool for the study of plant responses to an environmental changed.
(2) To analyze how light changes affect ion movement in rice, $^{28}Mg$, $^{32}P$, and $^{45}Ca$ were used.
(3) Stronger impact of light for P transport and almost no impact for Ca transport.
(4) The rate of P transport from sheath to blade was greatly influenced by light.
(5) The Ca transportation was not affected by light, suggesting that Ca movement is not influenced by water flow in xylem.

**Acknowledgements** This work was partly supported by JSPS KAKENHI Grant Number 15H02469 to T. M. Nakanishi, and 15k18761 to R. Sugita; the Japan Science and Technology Agency (JST) [PRESTO] (# 15665950) to K. Tanoi.

## References

1. Lazar T, Taiz L, Zeiger E (2003) Plant physiology. 3rd edn. Ann. Bot. Doi: 10.1093/aob/mcg079
2. Sakurai-Ishikawa J, Murai-Hatano M, Hayashi H, Ahamed A, Fukushi K, Matsumoto T, Kitagawa Y (2011) Transpiration from shoots triggers diurnal changes in root aquaporin expression. Plant Cell Environ. doi:10.1111/j.1365-3040.2011.02313.x
3. Fageria NK, Baligar VC, Clark R (2006) Physiology of crop production. CRC Press, Boca Raton
4. Orlich G (1998) Analysis of the driving forces of phloem transport in Ricinus seedlings: sucrose export and volume flow are determined by the source. Planta. doi:10.1007/s004250050399
5. Biddulph O, Cory R (1957) An analysis of translocation in the phloem of the bean plant using Tho, P(32), And C(14). Plant Physiol 32:608–619
6. Van Bel AJE (1976) Different mass transfer rates of labeled sugar and tritiated water in xylem vessels and their dependency on metabolism. Plant Physiol 57:911–914
7. Ohya T, Tanoi K, Hamada Y, Okabe H, Rai H, Hojo J, Suzuki K, Nakanishi T (2008) An analysis of long-distance water transport in the soybean stem using (H2O)-O-15. Plant Cell Physiol 49:718–729
8. Tanoi K, Hojo J, Nishioka M, Nakanishi T, Suzuki K (2005) New technique to trace [O-15]water uptake in a living plant with an imaging plate and a BGO detector system. J Radioanal Nucl Chem 263:547–552
9. Sugita R, Kobayashi NI, Hirose A, Saito T, Iwata R, Tanoi K, Nakanishi TM (2016) Visualization of mineral elements uptake and the dynamics of photosynthates in arabidopsis by a newly developed real-time radioisotope imaging system (RRIS). Plant Cell Physiol. doi:10.1093/pcp/pcw056
10. Marschner H (1995) Mineral nutrition of higher plants. Academic Press, New York
11. Kobayashi NI, Sugita R, Nobori T, Tanoi K, Nakanishi TM (2016) Tracer experiment using $^{42}K+$ and $^{137}Cs+$ revealed the different transport rates of potassium and caesium within rice roots. Funct Plant Biol. doi:10.1071/FP15245
12. Tanoi K, Kobayashi NI, Saito T, Iwata N, Hirose A, Ohmae Y, Iwata R, Suzuki H, Nakanishi TM (2013) Application of 28 Mg to the kinetic study of Mg uptake by rice plants. J Radioanal Nucl. doi:10.1007/s10967-012-2219-7
13. Sugita R, Kobayashi NI, Hirose A, Tanoi K, Nakanishi TM (2014) Evaluation of in vivo detection properties of $^{22}Na$, $^{65}Zn$, $^{86}Rb$, $^{109}Cd$ and $^{137}Cs$ in plant tissues using real-time radioisotope imaging system. Phys Med Biol. doi:10.1088/0031-9155/59/4/837
14. Kanno S, Yamawaki M, Ishibashi H, Kobayashi NI, Hirose A, Tanoi K, Nussaume L, Nakanishi TM (2012) Development of real-time radioisotope imaging systems for plant nutrient uptake studies. Philos Trans R Soc B. doi:10.1098/rstb.2011.0229
15. Hirose A, Yamawaki M, Kanno S, Igarashi S, Sugita R, Ohmae Y, Tanoi K, Nakanishi TM (2013) Development of a C-14

detectable real-time radioisotope imaging system for plants under intermittent light environment. J Radioanal Nucl. doi:10.1007/s10967-012-2130-2
16. Karley AJ, White PJ (2009) Moving cationic minerals to edible tissues: potassium, magnesium, calcium. Curr Opin Plant Biol 12:291–298
17. Biddulph O, Nakayama FS, Cory R (1961) Transpiration stream & ascension of calcium. Plant Physiol 36:429–436
18. Matsuo T, Kumazawa K, Ishii R, Ishihara K, Hirata H (1995) Science of the rice plant, vol 2. Physiology, Food and Agriculture Policy Research Center, Tokyo